

Supporting Information

One-step synthesis and self-assembly of luminescent sponge-like network of gold nanoparticles with high absorption capacity

Jiayi Zhu, Qian Lu, Chiyun Chen, Jianqiang Hu and Jinbin Liu*

Key Laboratory of Functional Molecular Engineering of Guangdong Province, School of Chemistry and Chemical Engineering, South China University of Technology, Guangzhou, China 510640.

Email: cejbliu@scut.edu.cn

Materials and equipment

Gold (III) chloride trihydrate (HAuCl_4) was purchased from Sigma-Aldrich (St Louis, MO, USA). Ethyl 3-mercaptopropanoate, butane-1,4-diylbis (3-mercaptopropanoate), 2-ethyl-2-(((3-mercaptopropanoyl)oxy)methyl)butane-1,4-diyl bis(3-mercaptopropanoate) and pentaerythritol tetrakis 3-mercaptopropionate (PTMP) were obtained from J&K Scientific Ltd. (Beijing, China). Cetyltrimethylammonium bromide (CTAB), sodium hydroxide (NaOH) and hydrochloric acid (HCl) were purchased from Zhi Yuan reagent Co., Ltd. (Tianjin, China). Nitric acid (HNO_3) was purchased from Enox (Jiangsu, China). All chemicals were used as received without further purification. Ultrapure water was achieved from a Milli-Q integral water purification system purchased from Millipore Corporation (Billerica, USA). Solutions of K (I), Na (I), Ca (II), Mg (II), Cr (III), Al (III), Ag (I), Cu (II), Zn (II), Ni (II), Co (III), Mn (II), Hg (II), Pb (II) and Fe (III) were prepared from KCl, NaCl, CaCl_2 , $\text{Mg}(\text{NO}_3)_2$, $\text{Cr}(\text{OAc})_3$, $\text{Al}(\text{NO}_3)_3$, AgNO_3 , CuSO_4 , $\text{Zn}(\text{OAc})_2$, $\text{Ni}(\text{Ac})_2$, $\text{Co}(\text{OAc})_3$, MnCl_2 , HgSO_4 , $\text{Pb}(\text{NO}_3)_2$ and $\text{Fe}(\text{NO}_3)_3$, respectively. Britton-Robinson (B-R) buffer solutions were prepared according to the standard protocols. All glassware was cleaned with fresh aqua regia ($\text{HCl}/\text{HNO}_3 = 3:1$, v/v) before use.

Luminescence spectra were recorded on a LS 55 luminescence spectrophotometer (PerkinElmer, USA) using 10 nm/10 nm slit widths for both excitation and emission measurements. UV-Vis absorption spectra were recorded on a UV-Vis Spectrophotometer UV-1780 (Shimadzu, Japan). FT-IR spectra were collected from 400 to 4000 cm^{-1} using a TENSOR 27 Fourier transform infrared (FT-IR) spectrometer (Bruker, Germany). The X-ray photoelectron spectroscopy (XPS) measurements were performed using a ESCALAB 250Xi instrument (Thermo Scientific, UK) with Al $\text{K}\alpha$ X-ray radiation (1486.6 eV) as excitation source, and C1s (284.8 eV) was used as reference energy for all binding energies. The photoluminescence quantum yields (QYs) were measured directly with the absolute QY measurement system C11347-11 (Hamamatsu Photonics K. K., Japan), equipped with an excitation light source and monochromator, an integrating sphere capable of nitrogen gas flow and a CCD spectrometer for detecting the whole spectral range simultaneously. This instrument was calibrated with fluorescein (QY, 88%) before the

measurements. Atomic force microscope (AFM) was carried out on a FSM-Nanoview 1000 (FSM-Precision, Suzhou) in tapping mode equipped with MikroMasch NSC11 AFM tip. All AFM images were processed with a freely software: WSxM 4.0 ([www. Nanotech.es](http://www.Nanotech.es)).⁴ Transmission electron microscopy (TEM) was carried out on a JEOL JEM 2100F TEM (Japan) with an accelerating voltage of 200 kV. Scanning electron microscope (SEM) was performed on a MERLIN compact field-emission SEM (Germany). The pH of all the solutions was measured by a Bante 902 pH meter (Shanghai, China). The Hg (II) concentrations were determined with a Prodigy High Dispersive inductively coupled plasma emission spectrometer (ICP-AES) from Teledyne Leeman (USA).

Elemental analysis

Elemental analysis showed that the sponge-like network of PTMP-AuNPs were composed of 28.49 % C, 3.205 % H and 16.9 % S. Chemical formulas of PTMP-AuNPs can be expressed as Au_xL_y , wherein L=PTMP containing a deprotonated thiol group ($C_{18}H_{26}O_8S_4$, 498.67 g/mol), x=number of Au atom, y=number of PTMP. The average ratio of Au-to-PTMP= x/y . The calculations of the ratios (x/y) from C, H and S elements were listed as follows:

Calculation of x/y using the measured mass fraction of C:

$$28.49 \% = 18yMr_C / (xMr_{Au} + yMr_L), \text{ and } x/y = 1.32;$$

1. Calculation of x/y using the measured mass fraction of H:

$$3.205 \% = 26yMr_H / (xMr_{Au} + yMr_L), \text{ and } x/y = 1.58;$$

2. Calculation of x/y using the measured mass fraction of S:

$$16.9 \% = yMr_S / (xMr_{Au} + yMr_L), \text{ and } x/y = 1.31;$$

3. Calculation of average the ratio of Au-to-PTMP (x/y):

$$(1.32 + 1.58 + 1.31) / 3 = 1.40.$$

Supplementary Data

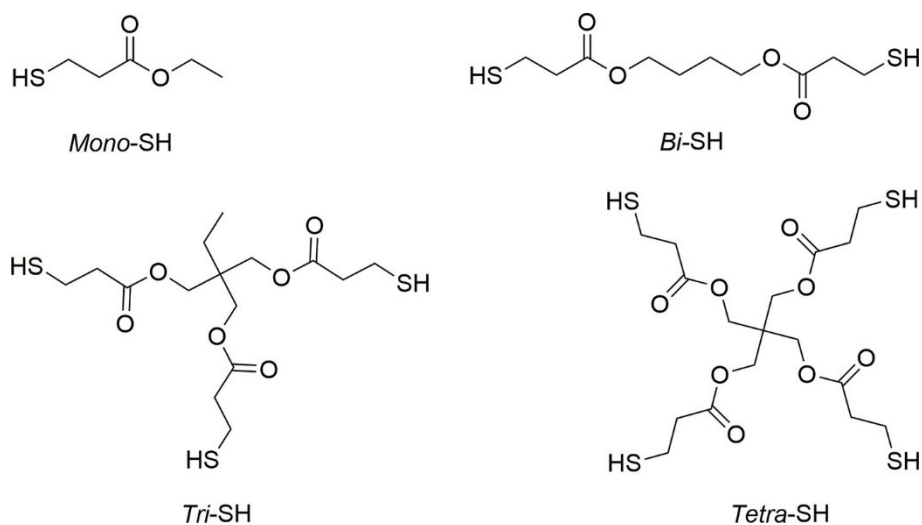


Fig. S1 Structures of the thiol ligands: ethyl 3-mercaptopropanoate (*Mono-SH*); butane-1,4-diyl bis(3-mercaptopropanoate) (*Bi-SH*); 2-ethyl-2-(((3-mercaptopropanoyl)oxy)methyl)butane-1,4-diyl bis(3-mercaptopropanoate) (*Tri-SH*); pentaerythritol tetrakis 3-mercaptopropionate (*Tetra-SH*).

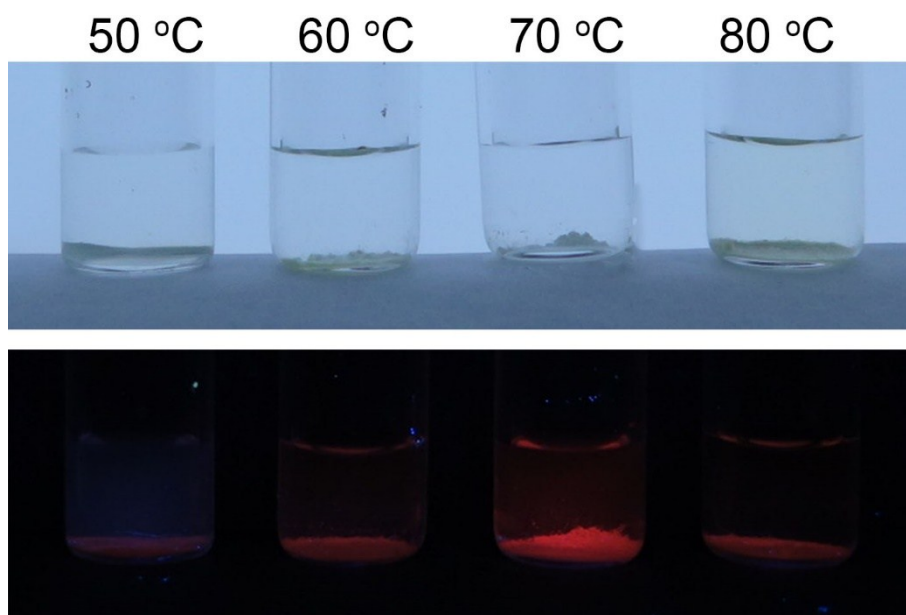


Fig. S2 Photographs of the assembled PTMP-AuNPs synthesized at different temperatures, and the pictures were taken under room light (upper panel) and 365-nm UV light (lower panel), respectively.

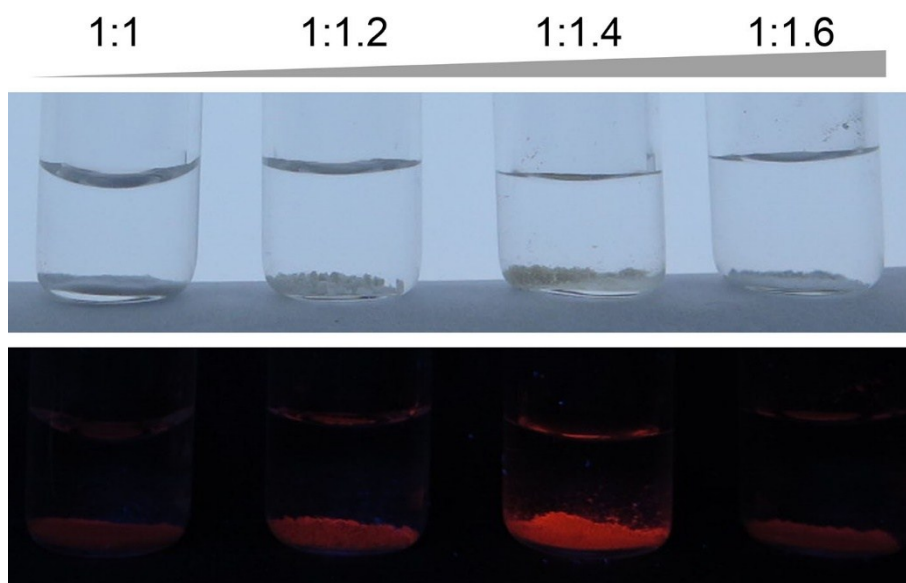


Fig. S3 Photographs of the assembled PTMP-AuNPs synthesized at 70 ° C with different molar ratios of PTMP to Au (III) (PTMP /Au (III)) after aging overnight, and the pictures were taken under room light (upper panel) and 365-nm UV light (lower panel), respectively.

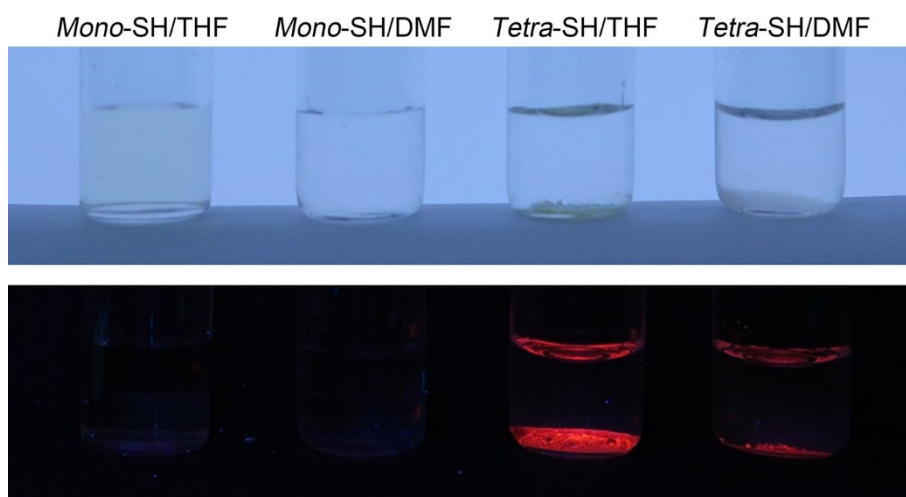


Fig. S4 Photographs of the assembled AuNPs dispersed in different organic solvents, and the pictures were taken under room light (upper panel) and 365-nm UV light (lower panel), respectively.

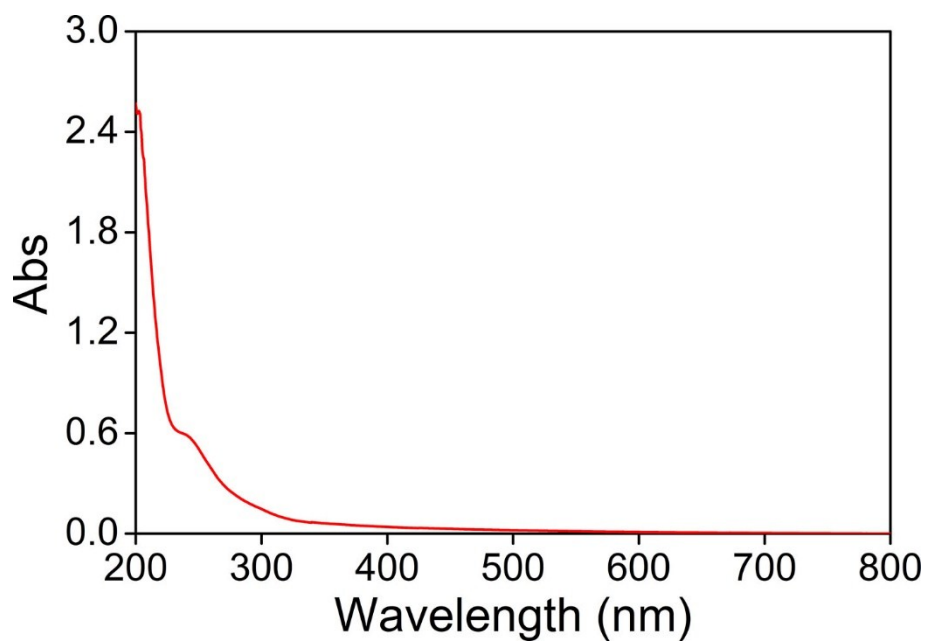


Fig. S5 The UV-Vis absorption spectrum of PTMP solution.

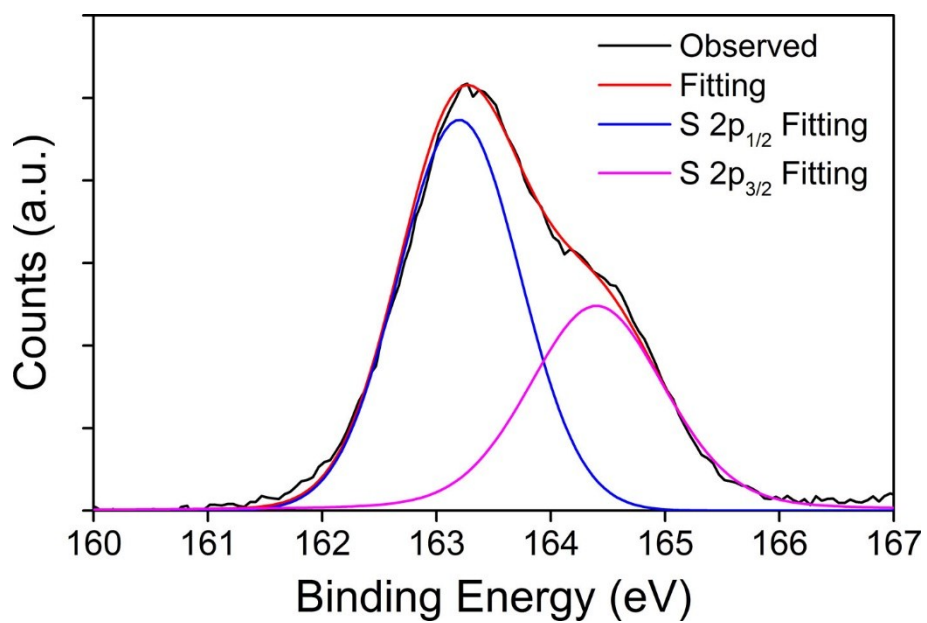


Fig. S6 XPS of S 2p spectrum of the sponge-like network of PTMP-AuNPs fitted with the binding energies of 163.1 and 164.2 eV, respectively.

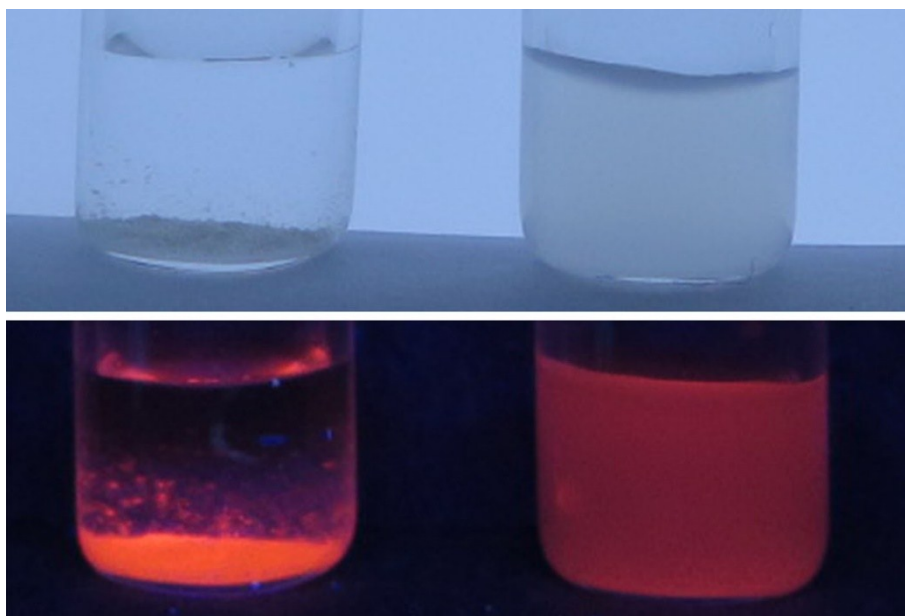


Fig. S7 Photographs of the sponge-like network of PTMP-AuNPs before (left) and after the CTAB dispersion under sonication (right), and the pictures were taken under room light (upper panel) and 365-nm UV light (lower panel), respectively.

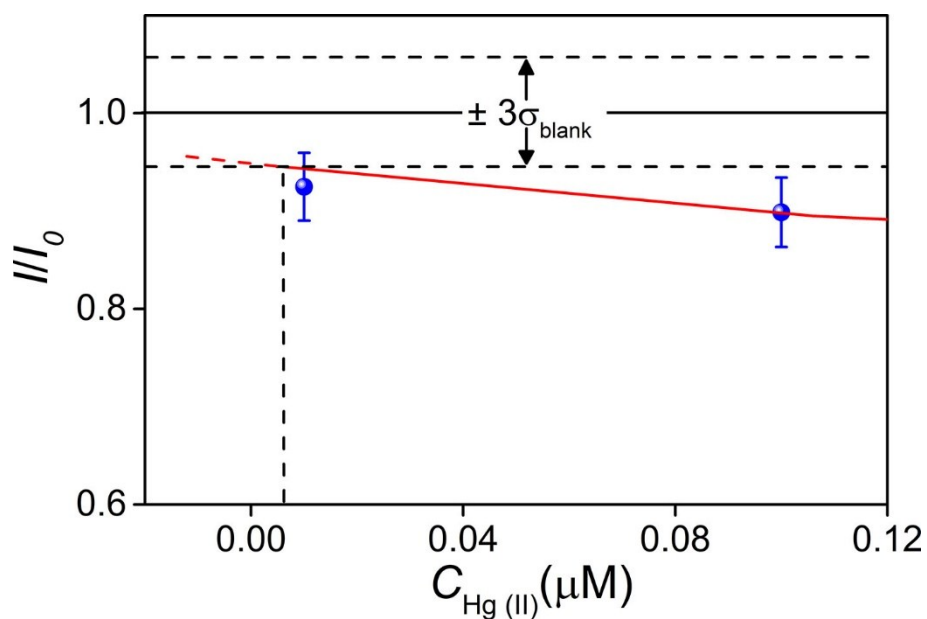


Fig. S8 A magnified graph of the calibration curve of Hg (II) at low concentrations less than 0.10 μM as showed in Figure 5b indicated that the limit of detection (LOD, 3δ) was calculated to be 6.0 nM.

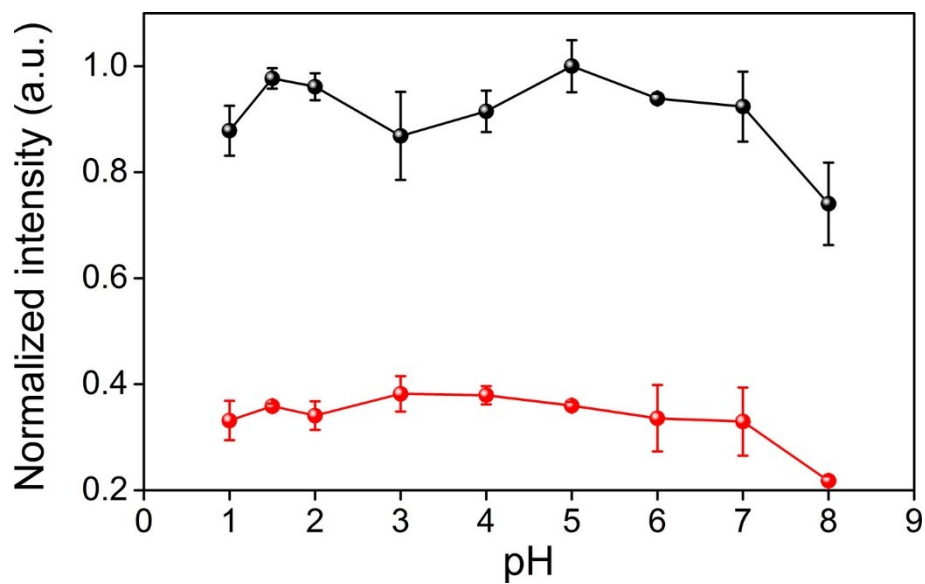


Fig. S9 Effect of pH on the luminescence intensities of the sponge-like network of PTMP-AuNPs at room temperature before (black) and after Hg (II) (50.0 μ M) incubation (red), respectively.

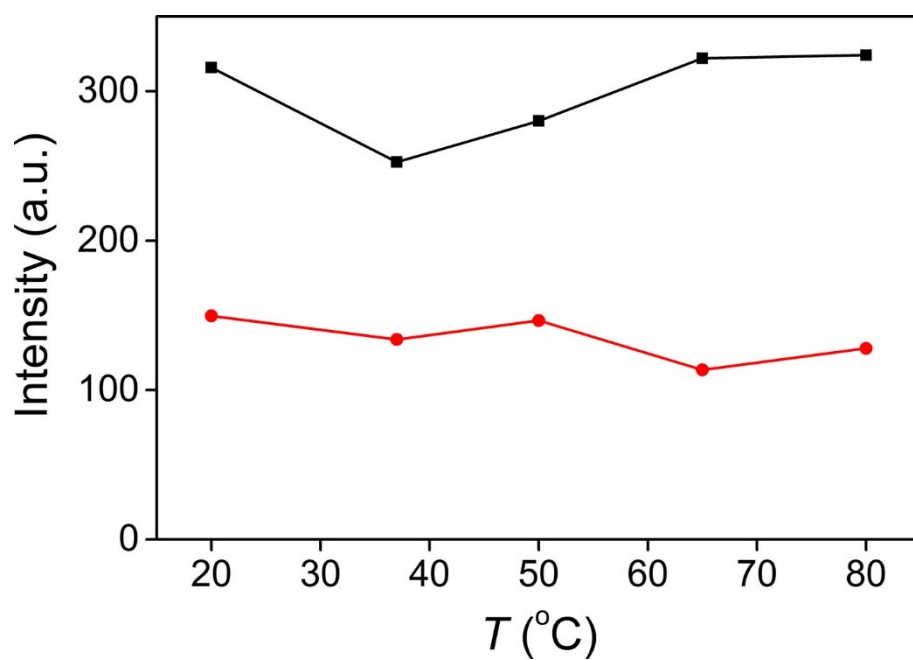


Fig. S10 Effect of temperature on the luminescence intensities of the sponge-like network of PTMP-AuNPs at pH 2.0 before (black) and after the incubation of Hg (II) (50.0 μ M) (red), respectively.

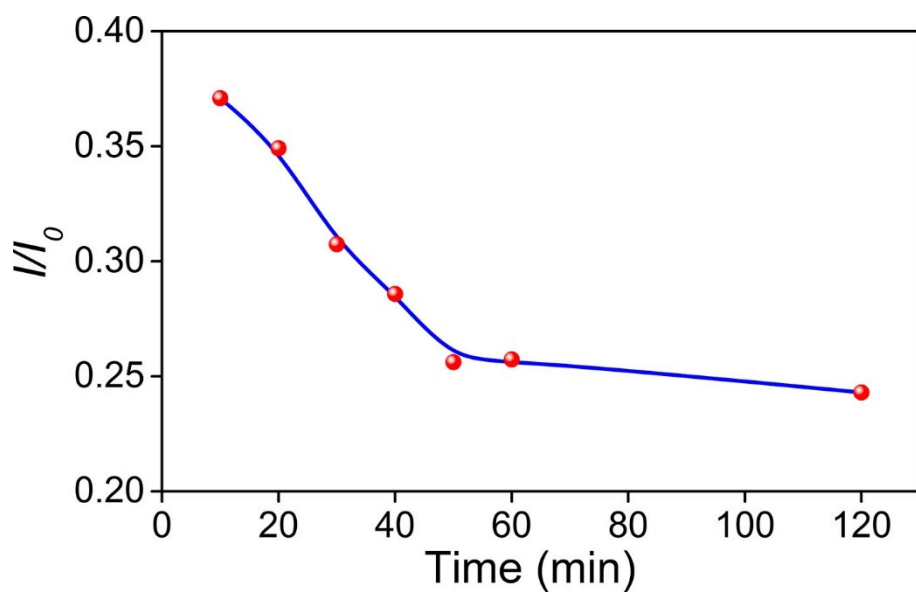


Fig. S11 The luminescence quenching efficiency (I/I_0) of the sponge-like network of PTMP-AuNPs after incubation with 0.10 mM Hg (II) measured at different time points.

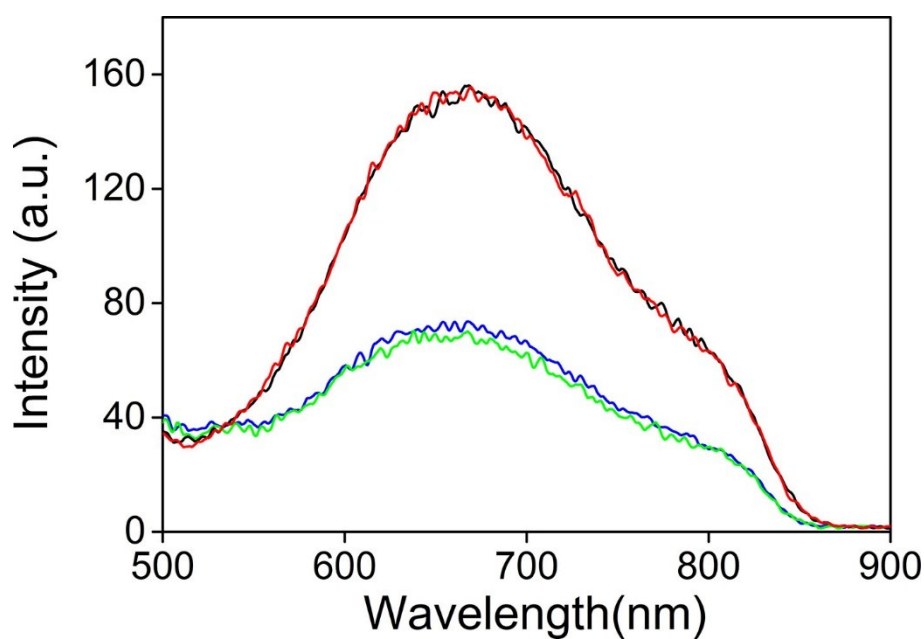


Fig. S12 Luminescence spectra of the synthesized sponge-like network of PTMP-AuNPs before (black) and after (blue) the incubation of Hg (II) ions (50.0 μ M), respectively. The addition of EDTA (0.1 mM) into the original PTMP-AuNPs (red) and the PTMP-AuNPs after incubation of Hg (II) ions (50.0 μ M, green), respectively.

References

- 1 Horcas, I.; Fernandez, R.; Gomez-Rodriguez, J. M.; Colchero, J.; Gomez-Herrero, J.; Baro, A. M. *Rev. Sci. Instrum.* 2007, **78**, 013705.